

Original citation:

Knox, Kirsten, Wang, Pengwei, Kriechbaumer, Verena, Tilsner, Jens, Frigerio, Lorenzo, Sparkes, Imogen, Hawes, Chris and Oparka, Karl, J.. (2015) Putting the squeeze on PDs - a role for RETICULONS in primary plasmodesmata formation. Plant Physiology . Article number 00668.2015.

Permanent WRAP url:

<http://wrap.warwick.ac.uk/68674>

Copyright and reuse:

The Warwick Research Archive Portal (WRAP) makes this work by researchers of the University of Warwick available open access under the following conditions. Copyright © and all moral rights to the version of the paper presented here belong to the individual author(s) and/or other copyright owners. To the extent reasonable and practicable the material made available in WRAP has been checked for eligibility before being made available.

Copies of full items can be used for personal research or study, educational, or not-for profit purposes without prior permission or charge. Provided that the authors, title and full bibliographic details are credited, a hyperlink and/or URL is given for the original metadata page and the content is not changed in any way.

Publisher's statement:

Published version: <http://dx.doi.org/10.1104/pp.15.00668>

Copyright © 2015 American Society of Plant Biologists. All rights reserved.

A note on versions:

The version presented here may differ from the published version or, version of record, if you wish to cite this item you are advised to consult the publisher's version. Please see the 'permanent WRAP url' above for details on accessing the published version and note that access may require a subscription.

For more information, please contact the WRAP Team at: publications@warwick.ac.uk

warwick**publications**wrap

highlight your research

<http://wrap.warwick.ac.uk>

1
2
3
4
5
6
7
8
9
10
11
12
13
14
15
16
17
18
19
20
21
22
23
24
25
26
27
28
29
30
31
32
33
34

Running Title: **Reticulons in primary plasmodesmata**

Author for correspondence: Prof. Karl Oparka
Regius Chair of Plant Science
Institute of Molecular Plant Science,
Rutherford Building,
University of Edinburgh,
Kings Buildings,
Mayfield Road,
Edinburgh
EH9 3BF
UK
karl.oparka@ed.ac.uk
+44 (0)131 650 7256

Research Area: Cell Biology

35
36 **Putting the squeeze on PDs – a role for RETICULONS in primary**
37 **plasmodesmata formation¹**
38
39 Kirsten Knox², Pengwei Wang^{2#}, Verena Kriechbaumer, Jens Tilsner, Lorenzo
40 Frigerio, Imogen Sparkes, Chris Hawes and Karl Oparka*
41
42 Institute of Molecular Plant Sciences, University of Edinburgh, Edinburgh EH9 3BF United Kingdom
43 (K.K., K.O.); Plant Cell Biology, Oxford Brookes University, Oxford, OX3 0BP, United Kingdom
44 (V.K., P.W, C.H.); Biomedical Sciences Research Complex, University of St Andrews, St Andrews,
45 KY16 9ST, United Kingdom (J.T); Life Sciences, University of Warwick, Coventry, CV4 7AL, United
46 Kingdom (L.F.); Biosciences, College of Life and Environmental Sciences, Geoffrey Pope Building,
47 University of Exeter, EX4 4QD United Kingdom (I.S).
48
49
50
51
52 Summary: Reticulon proteins involved in membrane curvature are targeted to the
53 developing cell plate and label desmotubules in developing primary plasmodesmata
54

55

56 ¹This work was supported by grant BB/J004987/1 from the British Biotechnology and
57 Biological Sciences Research Council (BBSRC) to K.O and C.H and by The
58 Leverhulme Trust (F/00 382/G) to C.H.

59

60 ² These authors contributed equally to the work.

61

62

63 [#] Current Address - School of Biological and Biomedical Sciences, Durham
64 University, Durham, DH1 3LE, United Kingdom.

65

66

67 * Author for correspondence, karl.oparka@ed.ac.uk

68

69

70 **Abstract**

71

72 Primary plasmodesmata (PD) arise at cytokinesis when the new cell plate forms.
73 During this process, fine strands of endoplasmic reticulum (ER) are laid down
74 between enlarging Golgi-derived vesicles to form nascent PD, each pore containing a
75 desmotubule, a membranous rod derived from the cortical ER. Little is known about
76 the forces that model the ER during cell-plate formation. Here we show that members
77 of the reticulon (RTNLB) family of ER-tubulating proteins may play a role in
78 formation of the desmotubule. RTNLB3 and RTNLB6, two RTNLBs present in the
79 PD proteome, are recruited to the cell plate at late telophase, when primary PD are
80 formed, and remain associated with primary PD in the mature cell wall. Both
81 RTNLBs showed significant co-localisation at PD with the viral movement protein of
82 tobacco mosaic virus, while super-resolution imaging (3D-SIM) of primary PD
83 revealed the central desmotubule to be labelled by RTNLB6. FRAP studies showed
84 that these RTNLBs are mobile at the edge of the developing cell plate, where new
85 wall materials are being delivered, but significantly less mobile at its centre where PD
86 are forming. A truncated RTNLB3, unable to constrict the ER, was not recruited to
87 the cell plate at cytokinesis. We discuss the potential roles of RTNLBs in
88 desmotubule formation.

89

90

91 **Introduction**

92

93 Plasmodesmata (PD), the small pores that connect higher plant cells, are complex
94 structures of about 50 nm in diameter. Each PD pore is lined by the plasma membrane
95 and contains an axial ER-derived structure known as the desmotubule (Overall and
96 Blackman, 1996; Maule, 2008; Tilsner et al., 2011). The desmotubule is an enigmatic
97 structure whose function has not been fully elucidated. The small spiralling space
98 between the desmotubule and the plasma membrane, known as the cytoplasmic sleeve,
99 is almost certainly a conduit for movement of small molecules (Oparka et al., 1999).
100 Some reports, however, suggest that the desmotubule may also function in cell-cell
101 trafficking, providing an ER-derived pathway between cells along which
102 macromolecules may diffuse (Cantrill et al., 1999). The desmotubule is one of the
103 most tightly constricted membrane structures found in nature (Tilsner et al., 2011) but
104 the forces that generate its intense curvature are not understood. In most PD, the
105 desmotubule is a tightly furled tube of about 15 nm in diameter in which the
106 membranes of the ER are in close contact along its length. The desmotubule may
107 balloon out in the region of the middle lamella into a central cavity, but at the neck
108 regions of the PD pore it is tightly constricted (Overall and Blackman, 1996; Ding et
109 al., 1992; Ehlers and Kollmann, 2001; Glockmann and Kollmann, 1996; Robinson-
110 Beers and Evert, 1991). Studies of PD using GFP targeted to the ER lumen (e.g. GFP-
111 HDEL) have shown that GFP is excluded from the desmotubule due to the
112 constriction of ER membranes in this structure (Oparka et al., 1999; Crawford and
113 Zambryski, 2000; Martens et al., 2006; Guenoune-Gelbart et al., 2008). Lumenal GFP
114 is therefore unable to move between plant cells unless the membranes of the
115 desmotubule become ‘relaxed’ in some way. On the other hand, dyes and some
116 proteins inserted into the ER membrane can apparently move through the
117 desmotubule, either along the membrane or through the lumen, at least under some
118 conditions (Grabski et al., 1993; Cantrill et al., 1999; Martens et al., 2006; Guenoune-
119 Gelbart et al., 2008).

120

121 Recently, a number of proteins have been described in mammalian, yeast and plant
122 systems that induce extreme membrane curvature. Among these are the
123 RETICULONS (RTN), integral membrane proteins that induce curvature of the ER to

124 form tubules (Voeltz et al., 2006; Hu et al., 2008; Sparkes et al., 2010; Tolley et al.,
 125 2008; 2010). In animals, RTNs have been shown to be involved in a wide array of
 126 endomembrane related processes including intracellular transport, vesicle formation
 127 and as RTNs can also influence axonal growth, they may have roles in neuro-
 128 degenerative disorders such as Alzheimers (Yang and Strittmatter, 2007). Arabidopsis
 129 has 21 RTN homologs, known as RTNLBs (Nziengui et al., 2007; Sparkes et al.,
 130 2010), considerably more than in yeast or mammals, but most have not been
 131 examined. RTNLBs contain two unusually long hydrophobic helices that form re-
 132 entrant loops (Voeltz et al., 2006; Hu et al., 2008; Sparkes et al., 2010; Tolley et al.,
 133 2010). These are thought to induce membrane curvature by the molecular wedge
 134 principle (Hu et al., 2008; Shibata et al., 2009). When RTNLBs are overexpressed
 135 transiently in cells expressing GFP-HDEL, the ER becomes tightly constricted and
 136 GFP-HDEL is excluded from the lumen of the constricted ER tubules (Tolley et al.,
 137 2008; 2010), a situation similar to that which occurs in desmotubules (Oparka et al.,
 138 1999; Crawford and Zambryski, 2000; Martens et al., 2006). *In vitro* studies with
 139 isolated membranes have shown that the degree of tubulation is proportional to the
 140 number and spacing of RTNLB proteins in the membrane (Hu et al., 2008). For
 141 example, to constrict the ER membrane into a structure of 15 nm, the diameter of a
 142 desmotubule, would require RTNLBs to be inserted every 2 nm or less along the
 143 desmotubule axis (Hu et al., 2008), potentially making the desmotubule an extremely
 144 protein-rich structure (Tilney et al., 1991). Interestingly, a number of RTNLB proteins
 145 appear in the recently described PD proteome (Fernandez-Calvino et al., 2011)
 146 suggesting that RTNLBs are good candidates for proteins that model the cortical ER
 147 into desmotubules.

148
 149 Primary PD form at cytokinesis during assembly of the cell plate (Hawes et al., 1981;
 150 Hepler, 1982). Of the numerous studies devoted to the structure of the cell plate, very
 151 few have examined the behaviour of the ER during cytokinesis. During mitosis,
 152 elements of ER are located in the spindle apparatus, separated from the cytoplasm
 153 (Hepler, 1980). Just prior to cytokinesis there is a relative paucity of ER in the region
 154 destined to become the cell plate (Hepler, 1980; Hawes et al. 1981). The studies of
 155 Hawes et al. (1981) and Hepler (1982), exploiting heavy-metal impregnation of the
 156 ER, showed that during the formation of the new cell plate strands of cortical ER are
 157 inserted across the developing wall, between the Golgi-derived vesicles that deposit

158 wall materials. These ER strands become increasingly thinner during formation of the
159 desmotubule, eventually excluding heavy metal stains from the ER lumen (Hepler,
160 1982). The centre of the desmotubule often appears electron-opaque in TEM images
161 and has been referred to as the ‘central rod’ (Overall and Blackman, 1996). This
162 structure may consist of proteins that extend from the inner ER leaflets, or may
163 correspond to head groups of the membrane lipids themselves. In the fully formed
164 primary PD, the desmotubule remains continuous with the cortical ER that runs close
165 to the new cell wall (Hawes et al., 1981; Hepler, 1982; Oparka et al., 1994).

166

167 Here we show that two of the RTNLBs present in the PD proteome, RTNLB3 and
168 RTNLB6, become localised to the cell plate during the formation of primary PD.
169 These RTNLBs remain associated with the desmotubule in fully formed PD and are
170 immobile, as evidenced by FRAP studies. A truncated version of RTNLB3, in which
171 the second hydrophobic region was deleted (Sparkes et al., 2010), was not recruited to
172 the cell plate at cytokinesis. We suggest that RTNLBs play an important role in the
173 formation of primary PD and discuss mechanisms by which these proteins may model
174 the ER into desmotubules.

175

176

177

178 **Results**

179

180 *RTNLBs appear at cell plates during cytokinesis*

181 Of the 21 RTNLB homologs in the Arabidopsis database, we generated transgenic
182 lines for RTNLBs 1-4 and 6, either as RTNLB-YFP or RTNLB-GFP fusions under
183 CaMV 35S promoters. In all transgenic lines, RTNLBs labelled the ER in interphase
184 cells (Fig. 1A-D). We noticed for some RTNLB lines that fluorescence became
185 localised to the cell plate in dividing root cells. This localisation was recorded for
186 RTNLBs 2, 3, 4 and 6 (Fig. 1E-H). In particular, strong cell-plate labelling was
187 observed for RTNLB3 and RTNLB6 (Fig. 1G & H), two RTNLBs present in the PD
188 proteome (Fernandez-Calvino et al., 2011).

189

190 To examine RTNLB distribution during cell division, we expressed Arabidopsis
191 RTNLB3 and RTNLB6 in tobacco BY2 cells and followed their distribution in
192 mitotically dividing cells. We used FM4-64 as a marker for the developing cell plate
193 (Bolte et al, 2004) and found that both RTNLBs showed strong co-localisation with
194 FM4-64 labelled cell-plate membranes (Fig. 1I & J). We found a strong signal
195 associated with the newly formed wall at the centre, and a more diffuse signal
196 associated with the trailing edges of the cell plate (Fig. 1I & J). Next, we expressed
197 the luminal ER marker GFP-HDEL together with RTNLB3-YFP. In BY2 cells at
198 interphase, as in Arabidopsis, GFP-HDEL is restricted to pockets in the ER by the
199 RTNLB3-YFP mediated constriction of the ER lumen (Fig S1A). However, both
200 RTNLB3-YFP and GFP-HDEL labelled the cortical ER uniformly throughout cell
201 division (Fig. 1K & L). However, RTNLB3 became redistributed from the cortical ER
202 into the developing cell plate during mid- and late-telophase, features not seen with
203 GFP-HDEL (Fig. 1L). We next agro-infiltrated constructs of RTNLB3-YFP and
204 RTNLB6-YFP into *Nicotiana benthamiana* plants transgenically expressing the
205 movement protein of tobacco mosaic virus fused to GFP (TMV.MP-GFP; Oparka et
206 al. 1999) that is known to locate to PD. In mature epidermal cells, we saw a
207 significant co-localisation of these RTNLB-fusions with MP-GFP (Fig. 2).

208

209 *Super-resolution imaging of primary PD*

210 To confirm that RTNLBs were associated with desmotubules we used 3D-structured
211 illumination microscopy (3D-SIM; see also Fitzgibbon et al., 2010) to examine

Figure 1

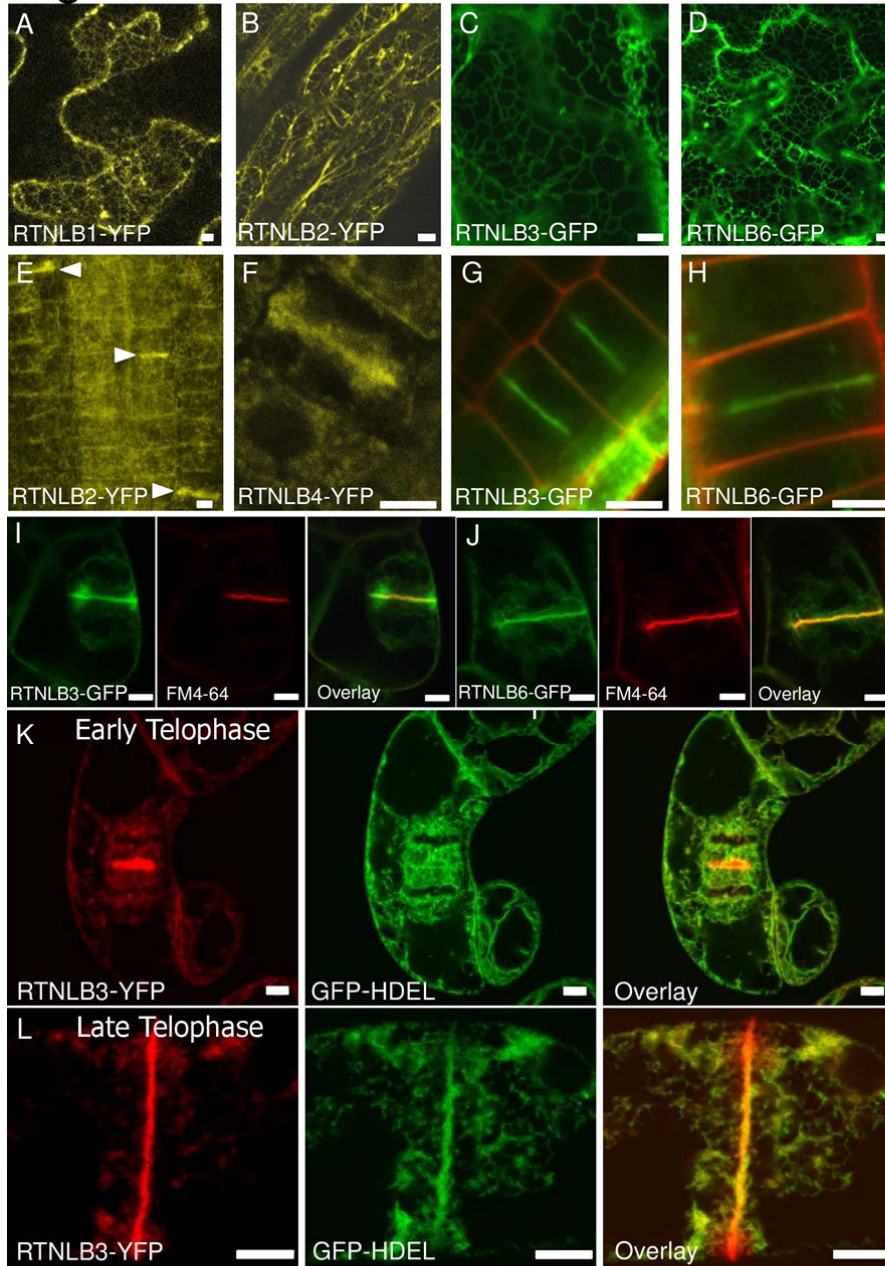


Figure 1

RETICULON localisation in Arabidopsis and Tobacco BY2 cells. RTNLBs label the ER but not the nuclear envelope in Arabidopsis leaf epidermis. **A**, RTNLB1-YFP **B**, RTNLB2-YFP **C**, RTNLB3-GFP **D**, RTNLB6-GFP. RTNLBs are recruited to the developing cell plate in Arabidopsis root cells **E**, RTNLB2-YFP **F**, RTNLB4-YFP **G**, RTNLB3-GFP **H**, RTNLB6-GFP. RTNLB3-GFP (**I**) and RTNLB6-GFP (**J**) are also recruited to the cell plate in BY2 cells. FM4-64 (red) strongly labels the cell plate. Overlaid images show that the RTNLB-GFP signal is more diffuse at the edges of the developing cell plate. RTNLB is recruited specifically from the cortical ER to the developing cell plate. During early telophase (**K**) RTNLB3-YFP and GFP-HDEL label both the cortical ER and the cell plate but by late telophase (**L**) RTNLB3 becomes redistributed into the cell plate. Bars = 5 μm.

212 primary PD in the walls between BY2 cells. To image the ER associated with PD
 213 more clearly, we plasmolysed adjacent cells expressing RTNLB3 or RTNLB6 and
 214 also imaged plasmolysed cells expressing RFP-HDEL for comparison. By confocal
 215 microscopy, we observed a strong RTNLB signal associated with punctae at the end

Figure 2

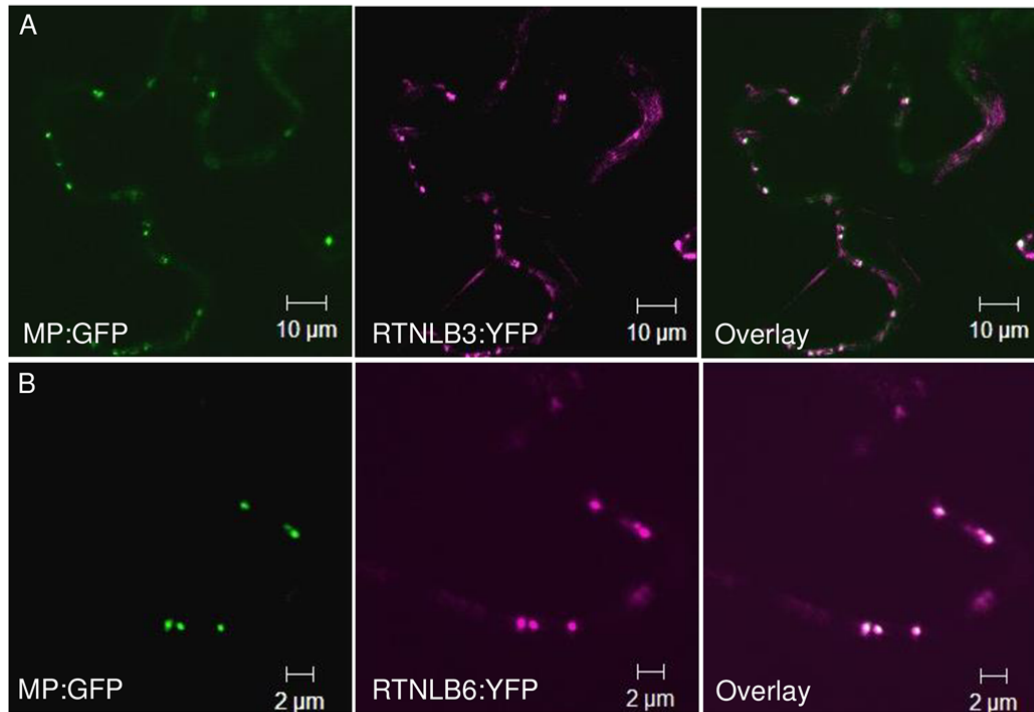


Figure 2

Co-localisation of the movement protein of tobacco mosaic virus (MP-GFP; green) with RTNLB3-YFP (A) and RTNLB6-YFP (B; magenta). Plasmodesmata showing co-localisation signals appear white.

216 walls of plasmolysed cells (Fig. 3A & B). Interestingly, Hechtian strands connecting
 217 the retracting protoplasts with the end walls showed strong RTNLB labelling,
 218 indicating that a constricted tubule of ER runs through each Hechtian strand (Fig. 3A
 219 & B). In contrast, we did not find RFP-HDEL within Hechtian strands or associated
 220 with PD (Fig. 3C), confirming previous reports that GFP targeted to the ER lumen is
 221 excluded from the centre of the desmotubule, where the ER membranes are in close
 222 contact (Oparka et al., 1999; Crawford and Zambryski, 2000; Martens et al., 2006;
 223 Guenoune-Gelbart et al., 2008). RFP-HDEL was also excluded from the Hechtian
 224 strands (Fig. 3C), indicating that during plasmolysis RFP-HDEL is ‘squeezed’ into
 225 the contracting protoplast.
 226
 227 With 3D-SIM we were able to resolve simple PD and found that desmotubules
 228 labelled with RTNLB6-GFP could be traced across individual cell walls (Fig. 3D-H).

Figure 3

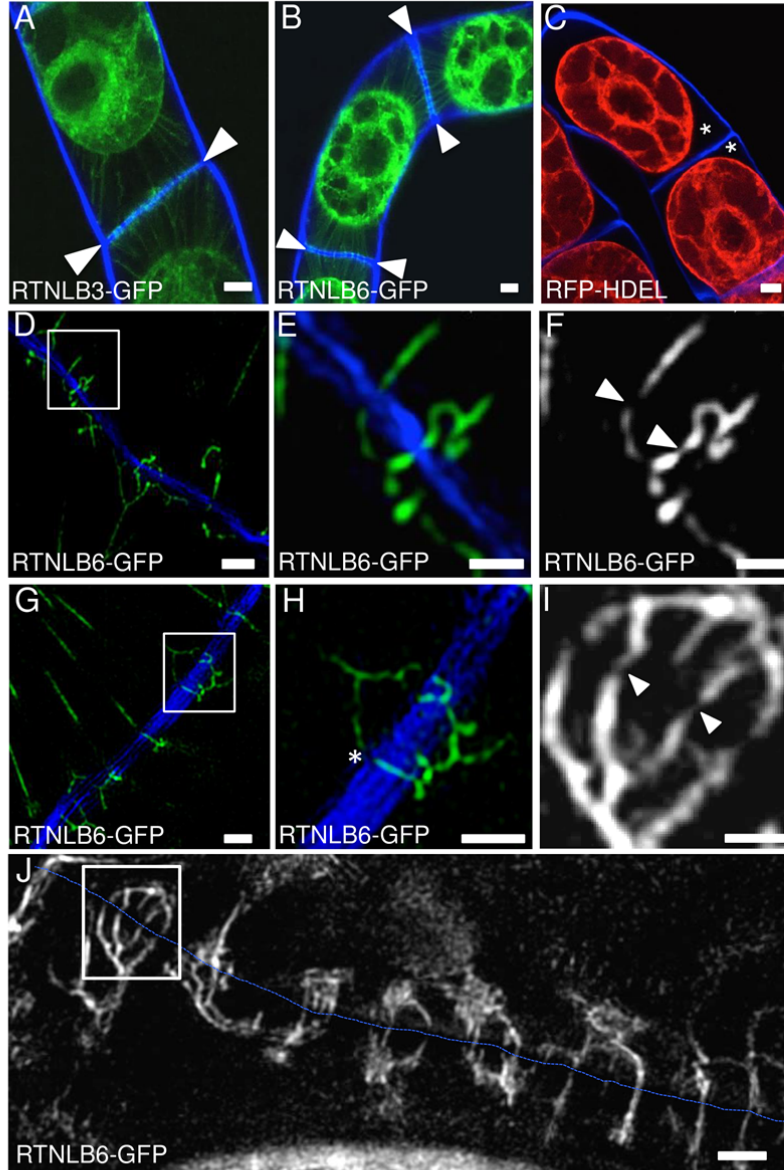


Figure 3

RTNLBs label the Hechtian strands of plasmolysed BY2 cells and show continuous labelling through PD. **A** and **B**, confocal images of RTNLB3-GFP (**A**) or RTNLB6-GFP (**B**) labelling of the Hechtian strands (green) in a plasmolysed BY2 cell. Calcofluor (blue) was used to visualise the cell wall between plasmolysed cells. GFP-labelled punctae were observed along the adjoining cell wall (darts), indicating the positions of PD. **C**, RFP-HDEL does not reveal the Hechtian strands or PD, leaving the space between the plasma membrane and cell wall unlabelled (*). **D-J**, 3D-SIM images of plasmolysed BY2 cells expressing RTNLB6-GFP. **D-F** RTNLB6-GFP labelled ER in Hechtian strands is severely constricted as it passes through PD. **E** and **F**, close up of boxed area in **D**, darts indicate areas of highly constricted ER, forming the desmotubule at the core of PD. **G** and **H**, the cortical ER shows abrupt changes in direction towards the entrance to a PD (*). **I**, single-channel close up of boxed region in **J**, showing the extreme constriction of the labelled ER. **J**, a section of the cell wall between cells (blue dashed line) showing that the RTNLB6-GFP labelled ER is continuous across the cell wall. Bars = 5 μm (A-C); 1 μm (D-I) and 0.5 μm (F).

229 Often we observed the cortical ER undergoing abrupt changes in direction towards
 230 the entrance of a PD pore (Fig. 3G & H). Fig. 3J shows the cortical ER associated
 231 with a single post-division wall. Note that multiple ER strands extend from the
 232 adjoining cells and converge at the entrances of plasmodesmata where they can be

233 traced across the wall. An enlargement of a region of cortical ER (Fig. 3I) shows that
234 desmotubules are labelled with RTNLB6. A movie depicting the 3-dimensional
235 arrangement of ER associated with PD is shown in supplementary movie 1. The
236 optical sections shown in supplementary Fig. S2 were taken 150 nm apart in the axial
237 dimension and show that a single RTNLB6-labelled desmotubule can be tracked as it
238 crosses the cell wall.

239

240 *FRAP reveals reduced RTNLB mobility during cell-plate formation*

241 We used fluorescence recovery after photobleaching (FRAP) to study the mobility of
242 RTNLBs in the developing cell plate. We compared the leading edge of the cell plate,
243 where the RTNLB signal was diffuse (Fig. 4B) with the middle of the cell plate where
244 RTNLB distribution was tightly confined (and where PD formation had presumably
245 begun; Hawes et al., 1981, Hepler, 1982). We found a higher rate of fluorescence
246 recovery at the edge of the cell plate compared to the centre, indicative of reduced
247 RTNLB mobility during the formation of primary PD (Fig. 4A). At the completion of
248 cytokinesis, we found that a strong RTNLB signal remained on the new cell wall (e.g.
249 Fig. 1L). We then plasmolysed BY2 cells expressing RTNLB3 or RTNLB6 and
250 performed FRAP on the ER associated with the primary PD in the cell wall. There
251 was no fluorescence recovery in this location, although ER in the centre of the cell
252 showed a characteristic fluorescence recovery (Fig. 4D). As BY2 cells often grow in
253 linear chains, we also photobleached the ER of entire cells and monitored the
254 bleached cell for fluorescence recovery. In this scenario, the only source of
255 fluorescence is from neighbouring cells, across the intervening PD (see also Grabski
256 et al., 1993). We failed to detect a return of fluorescence into the bleached cell,
257 indicating that even though RTNLBs are present in the desmotubule, this structure
258 does not form a conduit for RTNLB mobility between cells (Fig. 4E and F).

259

260 *A RTNLB truncation is not recruited to the developing cell plate*

261 Next, we utilised BY2 lines stably expressing a truncation of RTNLB3, comprising
262 the first two trans-membrane domains and cytosolic loop, but lacking the c-terminal
263 region predicted to form two transmembrane domains (RTNLB3t2; Sparkes et al,
264 2010). The ER in these cells was less tubular than in cells expressing the full length
265 protein (Fig S1B). This truncated protein was not strongly recruited to the cell plate at
266 cytokinesis and remained associated with the cytoplasmic ER (Fig. 5A and B). We

Figure 4

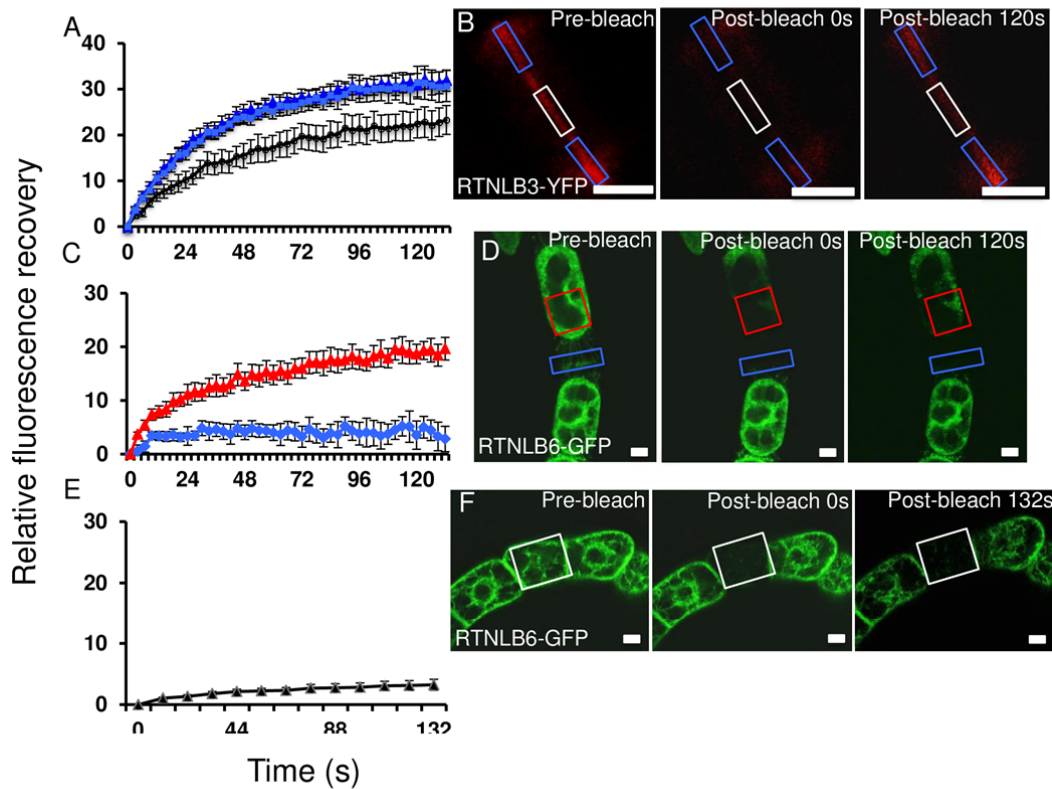


Figure 4

Fluorescence recovery after photobleaching (FRAP) reveals that RTNLB mobility is reduced in areas of PD development during cell plate formation.

A, FRAP comparing the leading edge of the developing cell plate (light and dark blue) with the centre of the cell plate (black diamonds) in BY2 cells expressing RTNLB3-YFP. **B** shows representative pre- and post-bleach images. Boxes indicate the bleached regions. **C**, RTNLB6-GFP on the ER associated with the primary PD at the cell wall in plasmolysed BY2 cells is immobile (blue diamonds), whereas within the protoplast, fluorescence recovers (red triangles) indicating RTNLB6-GFP mobility. **D** shows representative pre- and post-bleach images of RTNLB6-GFP labelled plasmolysed BY2 cells. Boxes indicate the bleached regions. **E**, whole cells bleached within a chain show that RTNLBs are not mobile between cells. **F** shows representative pre- and post-bleach images of RTNLB6-GFP labelled BY2 cells. Boxes indicate the bleached cell. Data are averages of at least 9 separate experiments and bars indicate standard error of the mean (SEM). Bars = 5 μ m.

then performed FRAP on cells expressing the RTNLB3t2. RTNLB3t2-YFP fluorescence in the cell plate of these cells recovered much more quickly than in those expressing the full-length RTNLB-YFP proteins (c.f. Fig. 5C with Fig. 4 A&B) and also at faster rates than luminal GFP-HDEL (Fig. 5C).

Figure 5

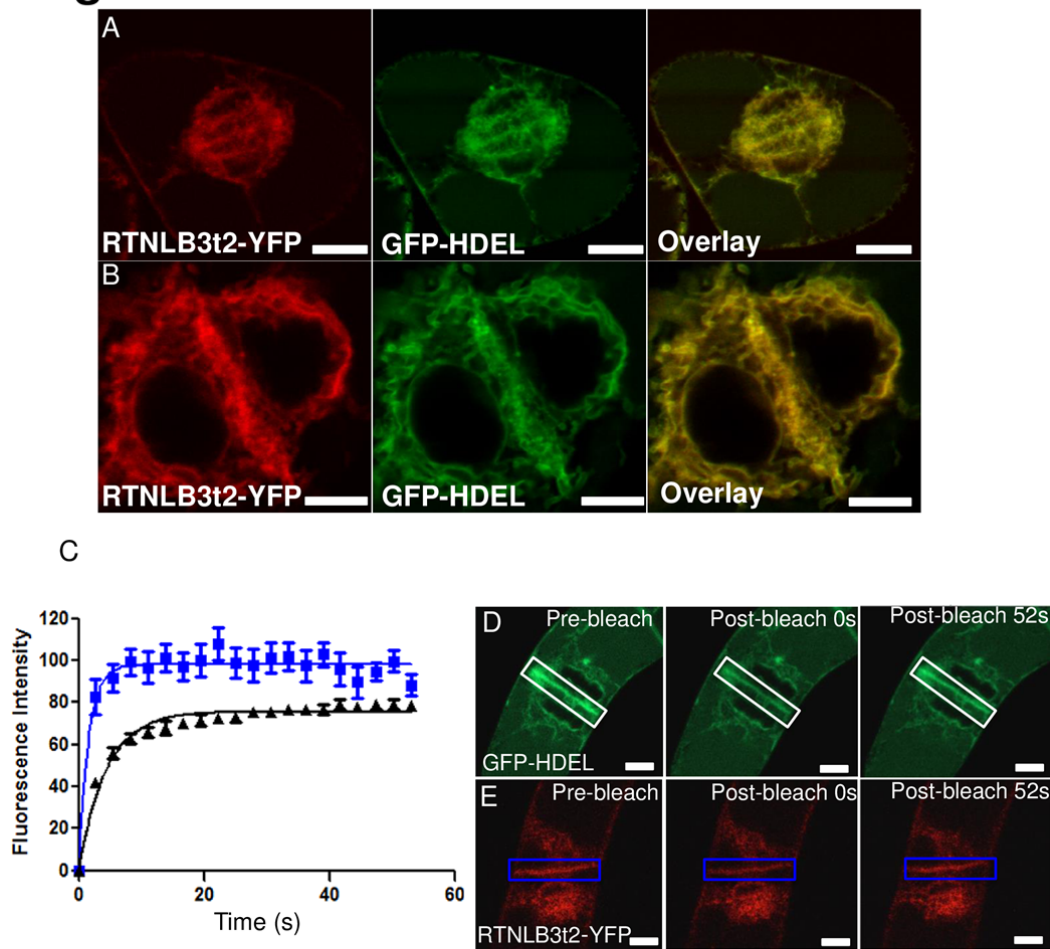


Figure 5

A truncated version of RTNLB3 (RTNLB3t2) is not recruited to the cell plate. **A** and **B** show RTNLB3t2-YFP co-expressed with GFP-HDEL. The overlaid images show that the RTNLB3t2 has even distribution across the ER, identical to GFP-HDEL, with no specific recruitment to the cell plate. **C**, FRAP of the cell plate in cells expressing RTNLB3t2-YFP showing that fluorescence recovers rapidly in the cell plate compared to GFP-HDEL and intact RTNLB3 (**D**, c.f. Fig.4 **A**). **D** and **E** represent pre- and post-bleach images. Bars = 5 μ m.

274 Discussion

275 The desmotubule, the intercellular strand of cortical ER that runs through
 276 plasmodesmata, is an extremely constricted membrane tubule whose function remains
 277 unclear. Proteins of the reticulon family are candidates for shaping the desmotubule as
 278 they constrict ER membranes and appear in the Arabidopsis PD proteome
 279 (Fernandez-Calvino et al., 2011). Here we present data suggesting that reticulons are
 280 indeed involved in modelling the cortical ER into desmotubules during the formation
 281 of primary PD. Of the seven Arabidopsis RTNLBs analysed so far, none were
 282 localised exclusively to PD, although both RTNLB3 and RTNLB6 were significantly

283 enriched at PD. The remainder were associated generally with the cortical ER
284 (Nziengui et al., 2007; Tolley et al., 2008; 2010; Sparkes et al., 2010; this study).
285 However, RTNLBs2-4 and RTNLB6 were recruited to the developing cell plate at
286 cytokinesis, where substantial ER modifications occur during PD formation. Of these
287 cell-plate localised reticulons, we focused on RTNLB3 and RTNLB6, both of which
288 are present in the PD proteome (Fernandez-Calvino et al., 2011).

289
290 Our 3D-SIM data show that RTNLB6 remains associated with the highly constricted
291 ER in primary PD of mature cell walls, and in Hechtian strands of plasmolysed cells.
292 Both of these ER regions allow diffusion of the membrane dye DiOC₆ (Grabski et al.,
293 1993; Oparka et al., 1994), but exclude luminal GFP-HDEL (Oparka et al., 1999;
294 Crawford and Zambryski, 2000; Martens et al., 2006; Guenoune-Gelbart et al., 2008).
295 Tolley et al. (2008; 2010) showed that over-expression of RTNLB13 constricted the
296 cortical ER to an extent that luminal GFP-HDEL was excluded, being forced into
297 luminal pockets distributed along tubules. Likewise the ER membrane marker GFP-
298 calnexin demonstrated that tubular ER could be constricted to fine threads (Sparkes et
299 al., 2010). Thus, there seems to be no *a priori* reason why RTNLBs could not form a
300 structure similar to the desmotubule. However, since the RTNLBs are distributed over
301 the entire cortical ER tubules, their presence alone cannot be sufficient to produce the
302 strong constriction of the desmotubule.

303
304 The degree of membrane constriction produced by RTNs is dependent on their
305 concentration (Hu et al., 2008). Our experiments provide no information on whether
306 or not RTNLBs are enriched within PD. However, the ability of RTNLBs to constrict
307 ER tubules depends on their oligomerisation, which in turn confers a loss of RTNLB
308 mobility (Shibata et al., 2009; Tolley et al., 2010). Significantly, we observed reduced
309 RTNLB3 and RTNLB6 mobility at the cell plate, and also in PD, as evidenced by
310 FRAP analysis. Although RTNLB3 and RTNLB6 labelling was continuous between
311 cells, no intercellular transport was detected, unlike that shown for the membrane dye
312 DiOC₆ (Grabski et al., 1993) and the ER transmembrane proteins calnexin, and ACA2
313 (Guenoune-Gelbart et al., 2008). Truncated RTNLB3 (RTNLB3t2) in which the C-
314 terminus proximal hydrophobic domain was deleted, a mutation that prevents
315 oligomerisation and membrane constriction (Tolley et al., 2010; Sparkes et al., 2010),
316 compromised recruitment to the cell plate and caused increased mobility on the plate

317 ER. The mobility of RTNLB3t2 was in fact greater than free luminal GFP, indicating
318 that the hydrophobic domain of RTNLB3 is likely required for the formation of low-
319 mobility oligomers (Tolley et al. 2010). Collectively, our data suggest that RTNLB3
320 and RTNLB6, and potentially other RTNLBs, oligomerise preferentially on those ER
321 strands that traverse the cell plate during the formation of desmotubules. The
322 positional cues that trigger this process remain unknown. RTNLBs1-7 form a cluster
323 of closely related isoforms (Nziengui et al., 2007, Tolley et al., 2008) but their
324 primary sequences contain no obvious clues as to why they should localise to the
325 developing cell plate. It is likely that interactions with other proteins present at the
326 cell plate and in PD may play a role in this context.

327

328 The desmotubule within PD often dilates in the middle lamella region of the wall,
329 creating a central cavity whose function is unknown. *In vitro*, the linear spacing of
330 RTNs determines the degree of dilation between the RTN insertion points, the greater
331 the distance between the constricting proteins the larger the membrane ‘bulge’ (Hu et
332 al., 2008). Absence or removal of RTNLBs from the central cavity region of PD could
333 provide a facile means of controlling ER dimensions within PD and may explain the
334 dilation of the desmotubule in the central cavity. In the case of secondary PD, which
335 form across already formed cell walls (Faulkner et al., 2008), RTNLBs may also play
336 a role in ER modelling as the cortical ER strands on either sides of the wall must meet
337 and fuse within secondary PD (Faulkner et al., 2008; Zhang & Hu, 2013).

338

339 In the electron microscope, globular proteins have been found along the length of the
340 desmotubule, associated with the outer ER leaflet (Hepler, 1982; Ding et al., 1992;
341 Ehlers and Kollmann, 2001). These have been suggested to be cytoskeletal elements
342 (Overall and Blackman, 1996), but it is equally possible that they are proteins such as
343 RTNLBs, responsible for maintaining the constriction of the desmotubule membranes
344 and also linking the desmotubule to the PM (see also Tilsner et al., 2011). Several
345 published electron micrographs show ‘spoke-like’ extensions between these proteins
346 and the plasma membrane (Ding et al., 1992, Schulz, 1995, Overall and Blackman,
347 1996; Ehlers and Kollmann, 2001). These links with the plasma membrane, as well as
348 other desmotubule-localised proteins, could contribute to a localised enrichment and
349 immobilisation of RTNLBs. The extensive protein scaffold of the desmotubule is
350 likely to impart considerable rigidity to this structure, and links to the plasma

Figure 6

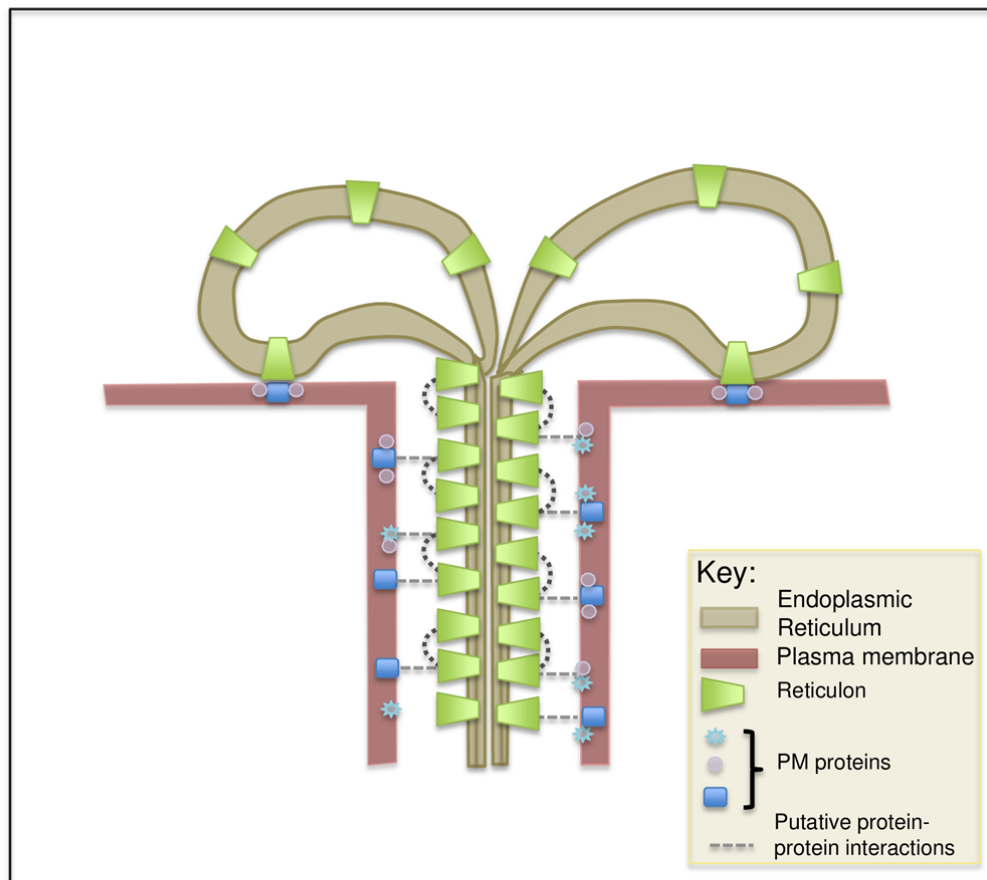


Figure 6

Model showing the insertion of RTNLB proteins into the membranes of the desmotubule. Putative protein-protein interactions between RTNLBs and proteins resident in the plasma membrane are depicted as broken lines.

351 membrane would provide a means of exerting control of PD size exclusion limit
 352 (Tilsner et al., 2011). A schematic showing the putative distribution of RTNLB
 353 proteins on the desmotubule, and their links with the PM, is shown in Figure 6. We
 354 are currently searching for interactors of RTNLBs that may fulfil the above functions.
 355
 356 Many of the viral movement proteins that facilitate virus transport through PD
 357 interact with the cortical ER, or are integral ER membrane proteins (Vilar et al., 2002;
 358 Krishnamurthy et al., 2003; Martinez-Gil et al., 2009; Peiro et al., 2014). The
 359 transmembrane movement proteins of *Potato virus X* accumulate in RTNLB-rich
 360 regions of curved cortical ER in yeast (Wu et al., 2011) and also in the desmotubules

361 of *Nicotiana benthamiana* PD (Tilsner et al., 2013). Viral movement proteins may
362 disrupt the desmotubule scaffold by perturbing protein-lipid or protein-protein
363 interactions (Tilsner et al. 2011). The links between viral proteins and desmotubule
364 proteins will be an interesting area for future research.

365

366 It remains to be shown how many of the RTNLB proteins in the Arabidopsis database
367 are involved in membrane curvature alone, and RTNLBs may have additional
368 functions at PD. A screen for proteins that interact with the FLAGELLIN
369 SENSITIVE2 (FLS2) receptor identified RTNLB1 and RTNLB2 as interacting
370 proteins, and these RTNLBs appear to regulate the transport of newly synthesised
371 FLS2 from the ER to the plasma membrane (Lee et al., 2011). FLS2 is also enriched
372 at PD (Faulkner et al., 2013). It will be interesting to determine whether other RTNLB
373 members play roles in either intra- or inter-cellular signalling.

374

375

376

377

378 **Materials and Methods**

379

380 **Plant material**

381

382 Arabidopsis seeds were sterilised with 10% (v/v) bleach, rinsed once in 70% (v/v)
383 ethanol and then rinsed four times in sterile ddH₂O. Unless otherwise stated seeds
384 were plated in petri dishes on Murashige and Skoog medium with 1% sucrose (w/v),
385 solidified with 1.2% (w/v) phytoagar and grown in 16-h photoperiods with 200 $\mu\text{E m}^{-2} \text{s}^{-1}$
386 at 18°C to 22°C.

387

388 **Molecular Biology and cloning**

389

390 The generation of both the RTNLB-YFP and the RTNLB3 truncation constructs have
391 previously been described (Sparkes et al 2010). RTNLB3 and RTNLB6 were
392 amplified by PCR from ABRC clones (ABRC), recombined into Gateway vector
393 pDONR201, and then both were recombined into binary vector pGWB405 creating c-
394 terminal GFP fusions (Nakagawa et al, 2007). All binary vectors were then

transformed into *Agrobacterium tumefaciens* GV3101 and thence into Arabidopsis (Col-0) using the floral dip method (Clough & Bent, 1998).

BY2 cell culture and transformation

Tobacco BY2 cells (*Nicotiana tabacum* cv BY-2 [Bright Yellow 2]) cell lines (Nagata et al, 1992) were cultured aseptically in liquid media containing 4.3 g l⁻¹ Murashige and Skoog Basal Media (Sigma, M5519), 200 µg ml⁻¹ 2,4-Dichlorophenoxyacetic acid and 30 g l⁻¹ sucrose. Cells were grown in the dark at 28°C on an orbital shaker and sub-cultured to fresh media weekly. RTNLB3-GFP and RTNLB6-GFP transgenic lines were generated by *Agrobacterium tumefaciens* mediated transformation with the binary vectors described above. 40µl of 20 mM acetosyringone was added to 40ml of 3 day old BY2 cell culture and cells were pipetted up and down 20 times to induce minor cell damage. The cells were then mixed with 100µl of the appropriate agrobacterium overnight culture and incubated at 28°C in the dark for 3 days. Cells were then washed 3 times in sterile media, resuspended in 5ml and plated on media solidified with 0.75% (w/v) phytoagar with 50µg ml⁻¹ cefotaxime and 50µg ml⁻¹ kanamycin. Plates were incubated for 3-4 weeks. Resultant calli were then sub-cultured onto fresh selective media to confirm antibiotic resistance before expression was assessed under fluorescence microscope and positive cell lines transferred and maintained in liquid culture. Cells were imaged at day 4 post sub-culture for cell plate studies and plasmolysis and day 4-6 for FRAP.

Confocal imaging and cell staining

Seedlings and BY2 cells were imaged live on slides using either a Leica SP2 Confocal Laser-Scanning Microscope (Leica Microsystems) with 40x and 63x water-immersion lens (HCX PLAPO CS; Leica Microsystems) or a Zeiss LSM510 Meta laser scanning confocal microscope with 40x or 63x oil immersion objectives. For cell plate images 3-day old Arabidopsis seedlings were partially synchronised by transferring to media containing 2 mM Hydroxyurea for 15-17 hours before imaging the roots. Arabidopsis roots were stained with 10µg ml⁻¹ propidium iodide, where

429 indicated. BY2 cells were stained with 8.5 $\mu\text{g ml}^{-1}$ Calcafluor White for 1h or 2 μM
430 FM4-64 (Synaptored) for 10 minutes and then media removed and replaced with fresh
431 before imaging or plasmolysis.

432

433

434 Plasmolysis experiments

435

436 BY2 cells were plasmolysed in a 0.45 M solution of Mannitol in liquid BY2 media
437 for 20 minutes, then mounted on slides in the osmoticum to maintain plasmolysis
438 throughout imaging.

439

440

441 Fluorescence Recovery after Photobleaching (FRAP)

442

443 FRAP analyses were conducted either on a a Zeiss LSM510 Meta Confocal Laser-
444 Scanning Microscope (Zeiss) or a Leica SP2 Confocal Laser-Scanning Microscope
445 (Leica Microsystems) under the 63x objective using rapid switching between low
446 intensity imaging and high intensity bleach mode. Pre and post bleach images were
447 collected using 40% intensity of the 488 laser. Bleaching of the selected region, either
448 an entire cell, a cell wall or square regions of interest (ROIs) on the middle or edges
449 of cell plates, was achieved with 5-10 scans at 100% intensity of the 488nm laser.
450 Subsequent recovery was monitored for up to 5 minutes, dependent on experiment.
451 Relative levels of fluorescence were normalised to the first post-bleach reading. Data
452 are the mean of at least 9 replicates with bars indicating the standard error of the mean
453 (SEM).

454

455

456

457 3D-SIM Microscopy

458

459 3D-SIM microscopy is fully described in Fitzgibbon et al., (2010) Briefly, the 3D-
460 SIM images were obtained using a Deltavision OMX Blaze microscope (GE
461 Healthcare) equipped with 405, 488 and 593 nm solid state lasers and a
462 UPlanSApochromat 100x 1.4 numerical aperture oil immersion objective (Olympus).

To maintain the delicate ER structure, BY2 cells were imaged live. Exposure times were typically between 100 and 200 ms, and the power of each laser was adjusted to achieve optimal intensities of between 1,000 and 3,000 counts in a raw image of 15-bit dynamic range of Edge sCMOS camera (PCO AG, Germany). As photobleaching of the GFP was an issue in the live cells, exposure times and laser power were adjusted to minimal levels. Unprocessed image stacks were composed of 15 images per z-section (five phase-shifted images per each of three interference pattern angles). Super-resolution three-dimensional image stacks were reconstructed with SoftWoRx 6.0 (GE) using channel specific OTFs and Wiener filter setting of 0.002 (0.005 for the DAPI channel) to generate a super-resolution three-dimensional image stack. Images from the different colour channels, recorded on separate cameras, were registered with SoftWorx 6.0 alignment tool (GE).

Accession Numbers

Sequence data for genes in this article can be found in GenBank/EMBL databases using the following accession numbers: RTNLB1, At4g23630; RTNLB2, At4g11220; RTNLB3, At1g64090; RTNLB4, At5g41600 and RTNLB6, At3g61560.

Acknowledgements

We are grateful for the technical expertise and assistance of Dr Markus Posch at the OMX facility, University of Dundee. Use of the OMX microscope was supported by an MRC Next Generational Optical Microscopy Award (MR/K015869/1).

Author Contributions

K.K, V.K, J.T, C.H and K.O designed research. K.K, P.W, V.K, J.T. L.F and I.S performed the research. K.K, P.W, V.K, C.H and K.O analysed the data. K.K, K.O wrote the paper.

497

498 **Figure Legends**

499

500 **Figure 1**

501 RETICULON localisation in Arabidopsis and Tobacco BY2 cells. RTNLBs label the
502 ER but not the nuclear envelope in Arabidopsis leaf epidermis. **A**, RTNLB1-YFP **B**,
503 RTNLB2-YFP **C**, RTNLB3-GFP **D**, RTNLB6-GFP. RTNLBs are recruited to the
504 developing cell plate in Arabidopsis root cells **E**, RTNLB2-YFP **F**, RTNLB4-YFP **G**,
505 RTNLB3-GFP **H**, RTNLB6-GFP. RTNLB3-GFP (**I**) and RTNLB6-GFP (**J**) are also
506 recruited to the cell plate in BY2 cells. FM4-64 (red) strongly labels the cell plate.
507 Overlaid images show that the RTNLB-GFP signal is more diffuse at the edges of the
508 developing cell plate. RTNLB is recruited specifically from the cortical ER to the
509 developing cell plate. During early telophase (**K**) RTNLB3-YFP and GFP-HDEL
510 label both the cortical ER and the cell plate but by late telophase (**L**) RTNLB3
511 becomes redistributed into the cell plate. Bars = 5 μ m.

512

513 **Figure 2**

514 Co-localisation of the movement protein of tobacco mosaic virus (MP-GFP; green)
515 with RTNLB3-YFP (**A**) and RTNLB6-YFP (**B**; magenta). Plasmodesmata showing
516 co-localisation signals appear white.

517

518

519 **Figure 3**

520 RTNLBs label the Hechtian strands of plasmolysed BY2 cells and show continuous
521 labelling through PD. **A** and **B**, confocal images of RTNLB3-GFP (**A**) or RTNLB6-
522 GFP (**B**) labelling of the Hechtian strands (green) in a plasmolysed BY2 cell.
523 Calcofluor (blue) was used to visualise the cell wall between plasmolysed cells. GFP-
524 labelled punctae were observed along the adjoining cell wall (darts), indicating the
525 positions of PD. **C**, RFP-HDEL does not reveal the Hechtian strands or PD, leaving
526 the space between the plasma membrane and cell wall unlabelled (*). **D-J**, 3D-SIM
527 images of plasmolysed BY2 cells expressing RTNLB6-GFP. **D-F** RTNLB6-GFP
528 labelled ER in Hechtian strands is severely constricted as it passes through PD. **E** and
529 **F**, close up of boxed area in **D**, darts indicate areas of highly constricted ER, forming
530 the desmotubule at the core of PD. **G** and **H**, the cortical ER shows abrupt changes in

direction towards the entrance to a PD (*). **I**, single-channel close up of boxed region in **J**, showing the extreme constriction of the labelled ER. **J**, a section of the cell wall between cells (blue dashed line) showing that the RTNLB6-GFP labelled ER is continuous across the cell wall. Bars = 5 μ m (A-C); 1 μ m (D-I) and 0.5 μ m (F).

Figure 4

Fluorescence recovery after photobleaching (FRAP) reveals that RTNLB mobility is reduced in areas of PD development during cell plate formation.

A, FRAP comparing the leading edge of the developing cell plate (light and dark blue) with the centre of the cell plate (black diamonds) in BY2 cells expressing RTNLB3-YFP. **B** shows representative pre- and post-bleach images. Boxes indicate the bleached regions. **C**, RTNLB6-GFP on the ER associated with the primary PD at the cell wall in plasmolysed BY2 cells is immobile (blue diamonds), whereas within the protoplast, fluorescence recovers (red triangles) indicating RTNLB6-GFP mobility. **D** shows representative pre- and post-bleach images of RTNLB6-GFP labelled plasmolysed BY2 cells. Boxes indicate the bleached regions. **E**, whole cells bleached within a chain show that RTNLBs are not mobile between cells. **F** shows representative pre- and post-bleach images of RTNLB6-GFP labelled BY2 cells. Boxes indicate the bleached cell. Data are averages of at least 9 separate experiments and bars indicate standard error of the mean (SEM). Bars = 5 μ m.

Figure 5

A truncated version of RTNLB3 (RTNLB3t2) is not recruited to the cell plate. **A** and **B** show RTNLB3t2-YFP co-expressed with GFP-HDEL. The overlaid images show that the RTNLB3t2 has even distribution across the ER, identical to GFP-HDEL, with no specific recruitment to the cell plate. **C**, FRAP of the cell plate in cells expressing RTNLB3t2-YFP showing that fluorescence recovers rapidly in the cell plate compared to GFP-HDEL and intact RTNLB3 (**D**, c.f. Fig.4 **A**). **D** and **E** representative pre- and post-bleach images. Bars = 5 μ m.

565

566 **Figure 6**

567 Model showing the insertion of RTNLB proteins into the membranes of the
568 desmotubule. Putative protein-protein interactions between RTNLBs and proteins
569 resident in the plasma membrane are depicted as broken lines.

570

571

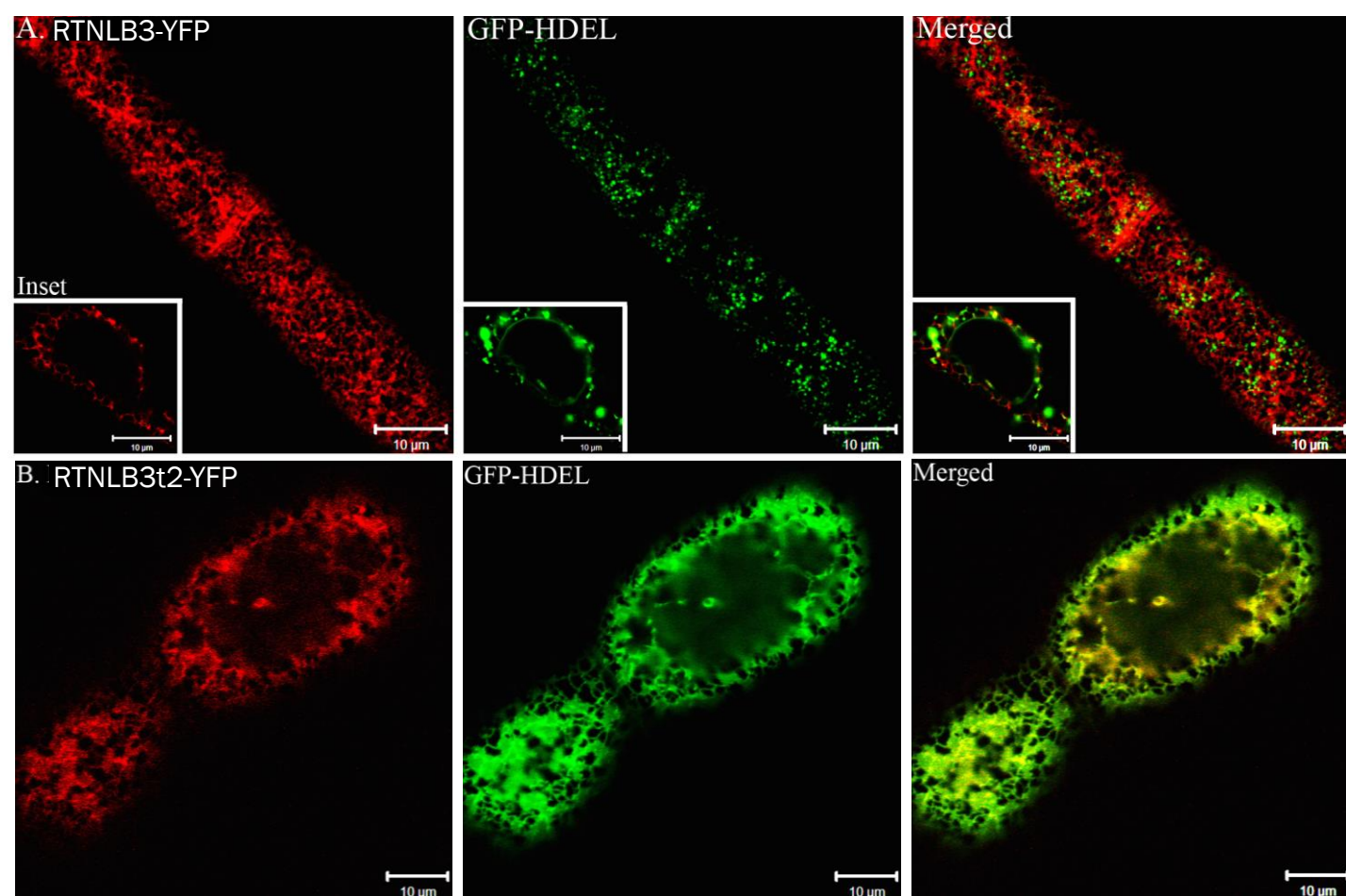
572

573

574

575

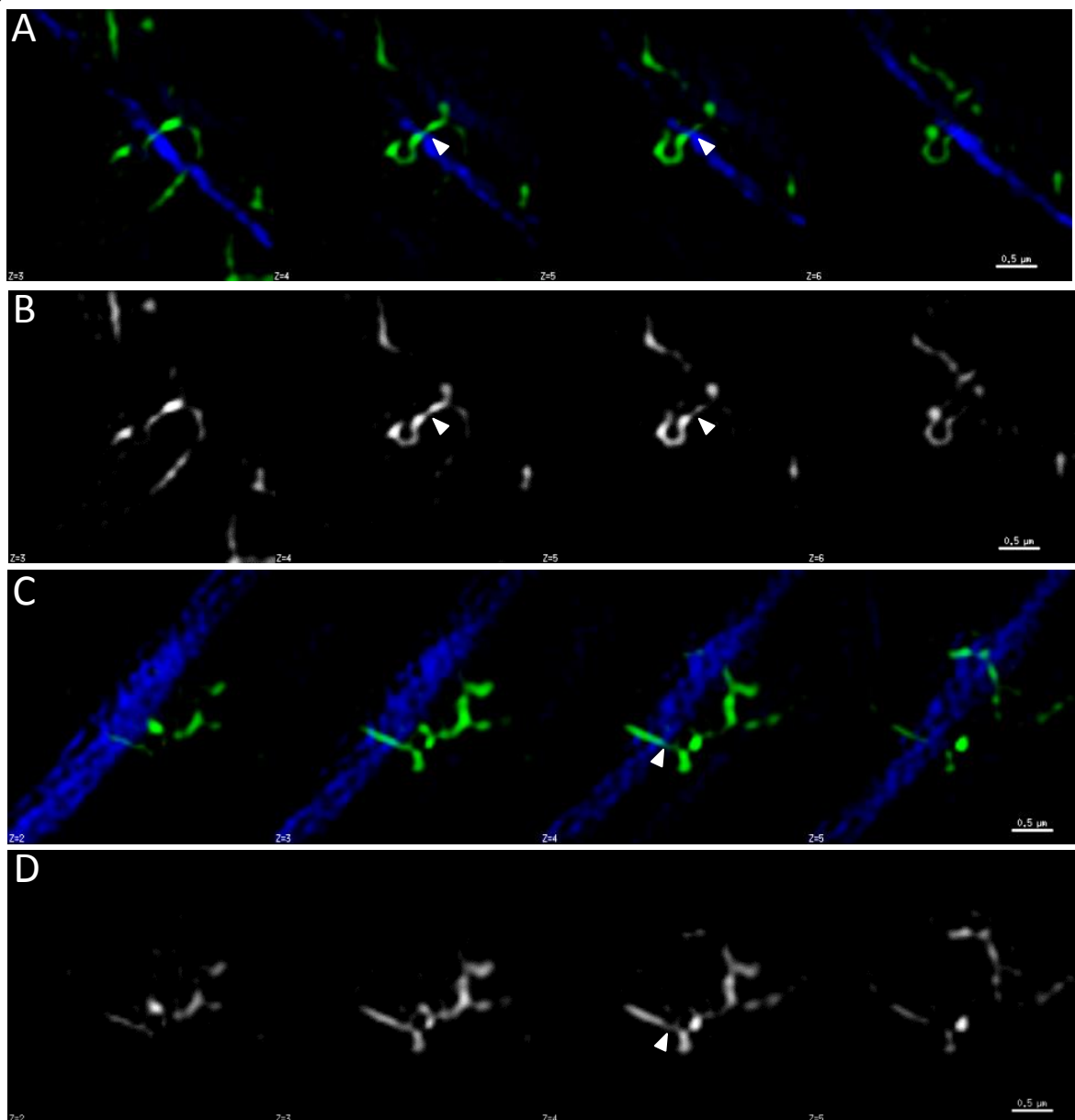
Figure S1



Supplementary Figure 1

RTNLB3-YFP can constrict the ER in interphase BY2 cells, whilst a truncated version cannot. A) GFP-HDEL is squeezed from the ER lumen into discrete luminal pockets when co-expressed with RTNLB3-YFP. Inset shows the nuclear envelope which has a low degree of curvature and is not labelled by RTNLB3. B) RTNLB3t2-YFP co-expressed with GFP-HDEL does not constrict the ER in BY2 cells.

Figure S2



Supplementary Figure 2

RTNLB6-GFP labels desmotubules in BY2 cells. Optical sections taken 150 nm apart in the axial dimension, show that a single desmotubule can be tracked as it crosses the cell wall. A and C) Series of sections showing RTNLB6-GFP (green) labelled ER is highly constricted as it passes through the cell wall (blue) B) Single channel of images in A or C, showing RTNLB6-GFP only. Bars = 0.5 μm .

Supplementary Video 1

Movie depicting a 3D reconstruction of ER (labelled with RTNLB6-GFP) associated with PD in BY2 cells.

Desmotubules can be seen as highly constricted regions crossing through the cell wall.

Parsed Citations

Bolte S, Talbot C, Boutte Y, Catrice O, Read ND, Satiat-Jeunemaitre B (2004) FM-dyes as experimental probes for dissecting vesicle trafficking in living plant cells. J Microscopy 214(2):159-173

Pubmed: [Author and Title](#)

CrossRef: [Author and Title](#)

Google Scholar: [Author Only](#) [Title Only](#) [Author and Title](#)

Cantrill LC, Overall RL, Goodwin PB (1999) Cell-to-cell communication via plant endomembranes. Cell Biol Int 23:653-661

Pubmed: [Author and Title](#)

CrossRef: [Author and Title](#)

Google Scholar: [Author Only](#) [Title Only](#) [Author and Title](#)

Clough SJ, Bent AF (1998) Floral dip: A simplified method for Agrobacterium-mediated transformation of Arabidopsis thaliana. Plant J 16(6):735-43

Pubmed: [Author and Title](#)

CrossRef: [Author and Title](#)

Google Scholar: [Author Only](#) [Title Only](#) [Author and Title](#)

Crawford KM, Zambryski PC (2000) Subcellular localization determines the availability of non-targeted proteins to plasmodesmatal transport. Curr Biol 10:1032-1040

Pubmed: [Author and Title](#)

CrossRef: [Author and Title](#)

Google Scholar: [Author Only](#) [Title Only](#) [Author and Title](#)

Ding B, Turgeon R, Parthasarathy MV (1992) Substructure of freeze-substituted plasmodesmata. Protoplasma 169:28-41

Pubmed: [Author and Title](#)

CrossRef: [Author and Title](#)

Google Scholar: [Author Only](#) [Title Only](#) [Author and Title](#)

Ehlers K, Kollmann R (2001) Primary and secondary plasmodesmata: structure, origin and functioning. Protoplasma 216:1-30

Pubmed: [Author and Title](#)

CrossRef: [Author and Title](#)

Google Scholar: [Author Only](#) [Title Only](#) [Author and Title](#)

Faulkner C, Akman OE, Bell K, Jeffree C, Oparka K (2008) Peeking into pit fields: a multiple twinning model of secondary plasmodesmata formation in tobacco. Plant Cell 20:1504-1518

Pubmed: [Author and Title](#)

CrossRef: [Author and Title](#)

Google Scholar: [Author Only](#) [Title Only](#) [Author and Title](#)

Faulkner C, Petutschnig E, Benitez-Alfonso Y, Beck M, Robatzek S, Lipka V, Maule AJ (2013) LYM2-dependent chitin perception limits molecular flux via plasmodesmata. Proc Natl Acad Sci USA 110(22):9166-70

Pubmed: [Author and Title](#)

CrossRef: [Author and Title](#)

Google Scholar: [Author Only](#) [Title Only](#) [Author and Title](#)

Fernandez-Calvino L, Faulkner C, Walshaw J, Saalbach G, Bayer E, Benitez-Alfonso Y, Maule A (2011) Arabidopsis plasmodesmal proteome. PLoS One 6(4):e18880

Pubmed: [Author and Title](#)

CrossRef: [Author and Title](#)

Google Scholar: [Author Only](#) [Title Only](#) [Author and Title](#)

Fitzgibbon J, Bell K, King E, Oparka K (2010) Super-resolution imaging of plasmodesmata using three-dimensional structured illumination microscopy. Plant Physiol 153(4):1453-63

Pubmed: [Author and Title](#)

CrossRef: [Author and Title](#)

Google Scholar: [Author Only](#) [Title Only](#) [Author and Title](#)

Glockmann C, Kollmann R (1996) Structure and development of cell connections in the phloem of Metasequoia glyptostroboides needles I. Ultrastructural aspects of modified primary plasmodesmata in Strasburger cells. Protoplasma 193:191-203

Pubmed: [Author and Title](#)

CrossRef: [Author and Title](#)

Google Scholar: [Author Only](#) [Title Only](#) [Author and Title](#)

Grabski S, de Feijter AW, Schindler M (1993) Endoplasmic reticulum forms a dynamic continuum for lipid diffusion between contiguous soybean root cells. Plant Cell 5:25-38

Pubmed: [Author and Title](#)

CrossRef: [Author and Title](#)

Google Scholar: [Author Only](#) [Title Only](#) [Author and Title](#)

Guenoun-Gelbart D, Elbaum M, Sagi G, Levy A, Epel BL (2008) Tobacco mosaic virus (TMV) replicase and movement protein function synergistically in facilitating tmv spread by lateral diffusion in the plasmodesmal desmotubule of Nicotiana benthamiana. Mol Plant Microb Interact 21:335-345

Pubmed: [Author and Title](#)

CrossRef: [Author and Title](#)

Google Scholar: [Author Only](#) [Title Only](#) [Author and Title](#)

Hawes CR, Juniper BE, Horne JC (1981) Low and high voltage electron microscopy of mitosis and cytokinesis in maize roots. Planta 152:397-407

Pubmed: [Author and Title](#)
CrossRef: [Author and Title](#)
Google Scholar: [Author Only](#) [Title Only](#) [Author and Title](#)

Hepler PK (1980) Membranes in the mitotic apparatus of barley cells. J Cell Biol 86(2):490-9

Pubmed: [Author and Title](#)
CrossRef: [Author and Title](#)
Google Scholar: [Author Only](#) [Title Only](#) [Author and Title](#)

Hepler PK (1982) Endoplasmic reticulum in the formation of the cell plate and plasmodesmata. Protoplasma 111:121-133

Pubmed: [Author and Title](#)
CrossRef: [Author and Title](#)
Google Scholar: [Author Only](#) [Title Only](#) [Author and Title](#)

Hu J, Shibata Y, Voss C, Shemesh T, Li Z, Coughlin M, Kozlov MM, Rapoport TA, Prinz WA (2008) Membrane proteins of the endoplasmic reticulum induce high-curvature tubules. Science 319:1247-1250

Pubmed: [Author and Title](#)
CrossRef: [Author and Title](#)
Google Scholar: [Author Only](#) [Title Only](#) [Author and Title](#)

Krishnamurthy K, Heppler M, Mitra R, Blancaflor E, Payton M, Nelson RS, Verchot-Lubicz J (2003) The Potato virus X TGBp3 protein associates with the ER network for virus cell-to-cell movement. Virology 309:269-281

Pubmed: [Author and Title](#)
CrossRef: [Author and Title](#)
Google Scholar: [Author Only](#) [Title Only](#) [Author and Title](#)

Lee HY, Bowen CH, Popescu GV, Kang HG, Kato N, Ma S, Dinesh-Kumar S, Snyder M, Popescu SC (2011) Arabidopsis RTNLBLB1 and RTNLBLB2 reticulon-like proteins regulate intracellular trafficking and activity of the FLS2 immune receptor. Plant Cell 23(9):3374-91

Pubmed: [Author and Title](#)
CrossRef: [Author and Title](#)
Google Scholar: [Author Only](#) [Title Only](#) [Author and Title](#)

Martínez-Gil L, Sánchez-Navarro JA, Cruz A, Pallas V, Pérez-Gil J, Mingarro I (2009) Plant virus cell-to-cell movement is not dependent on the transmembrane disposition of its movement protein. J Virol 83:5535-5543

Pubmed: [Author and Title](#)
CrossRef: [Author and Title](#)
Google Scholar: [Author Only](#) [Title Only](#) [Author and Title](#)

Maule AJ (2008) Plasmodesmata: structure, function and biogenesis. Curr Opin Plant Biol 11:680-686

Pubmed: [Author and Title](#)
CrossRef: [Author and Title](#)
Google Scholar: [Author Only](#) [Title Only](#) [Author and Title](#)

Martens HJ, Roberts AG, Oparka KJ, Schulz A (2006) Quantification of plasmodesmatal endoplasmic reticulum coupling between sieve elements and companion cells using fluorescence redistribution after photobleaching. Plant Physiol 142:471-480

Pubmed: [Author and Title](#)
CrossRef: [Author and Title](#)
Google Scholar: [Author Only](#) [Title Only](#) [Author and Title](#)

Nagata T, Nemoto Y, Hasezawa S (1992) Tobacco BY-2 cell line as the "He-La" cell in the cell biology of higher plants. Int Rev Cyt 132:1-30

Pubmed: [Author and Title](#)
CrossRef: [Author and Title](#)
Google Scholar: [Author Only](#) [Title Only](#) [Author and Title](#)

Nakagawa T, Kurose T, Hino T, Tanaka K, Kawamukai M, Niwa Y, Toyooka K, Matsuoka K, Jinbo T and Kimura T (2007) Development of series of gateway binary vectors, pGWBs, for realizing efficient construction of fusion genes for plant transformation. J Biosci Bioeng 104(1):34-41

Pubmed: [Author and Title](#)
CrossRef: [Author and Title](#)
Google Scholar: [Author Only](#) [Title Only](#) [Author and Title](#)

Nziengui H, Bouhidel K, Pillon D, Der C, Marty F, Schoefs B (2007) Reticulon-like proteins in Arabidopsis thaliana: structural organization and ER localization. FEBS Lett 581:3356-3362

Pubmed: [Author and Title](#)
CrossRef: [Author and Title](#)
Google Scholar: [Author Only](#) [Title Only](#) [Author and Title](#)

Oparka KJ, Prior DAM, Crawford JW (1994) Behavior of plasma-membrane, cortical ER and plasmodesmata during plasmolysis of onion epidermal-cells. Plant Cell Environ 17:163-171

Pubmed: [Author and Title](#)
CrossRef: [Author and Title](#)
Google Scholar: [Author Only](#) [Title Only](#) [Author and Title](#)

Oparka KJ, Roberts AG, Boevink P, Santa Cruz S, Roberts IM, Pradel KS, Imlau A, Kotlizky G, Sauer N, EpeI BL (1999) Simple, but not branched, plasmodesmata allow the nonspecific trafficking of proteins in developing tobacco leaves. Cell 97:743-754

Pubmed: [Author and Title](#)
CrossRef: [Author and Title](#)
Google Scholar: [Author Only](#) [Title Only](#) [Author and Title](#)

Overall RL, Blackman LM (1996) A model of the macro-molecular structure of plasmodesmata. Trends Plant Sci 1:307-311

Pubmed: [Author and Title](#)

CrossRef: [Author and Title](#)

Google Scholar: [Author Only](#) [Title Only](#) [Author and Title](#)

Peiro A, Martinez-Gil L, Tamborero S, Pallas V, Sanchez-Navarro JA, Mingarro I (2014) The tobacco mosaic virus movement protein associates with but does not integrate into biological membranes. J Virol 88(5):3016-26

Pubmed: [Author and Title](#)

CrossRef: [Author and Title](#)

Google Scholar: [Author Only](#) [Title Only](#) [Author and Title](#)

Robinson-Beers K, Evert RF (1991) Fine structure of plasmodesmata in mature leaves of sugarcane. Planta 184:307-318

Pubmed: [Author and Title](#)

CrossRef: [Author and Title](#)

Google Scholar: [Author Only](#) [Title Only](#) [Author and Title](#)

Schulz A (1995) Plasmodesmal widening accompanies the short-term increase in symplasmic phloem unloading in pea root-tips under osmotic stress. Protoplasma 188: 22-37

Pubmed: [Author and Title](#)

CrossRef: [Author and Title](#)

Google Scholar: [Author Only](#) [Title Only](#) [Author and Title](#)

Shibata Y, Hu J, Kozlov MM, Rapoport TA (2009) Mechanisms shaping the membranes of cellular organelles. Annu Rev Cell Dev Biol 25:329-54

Pubmed: [Author and Title](#)

CrossRef: [Author and Title](#)

Google Scholar: [Author Only](#) [Title Only](#) [Author and Title](#)

Sparkes IA, Tolley N, Aller I, Svozil J, Osterrieder A, Botchway S, Mueller C, Frigerio L, Hawes C (2010) Five arabidopsis reticulon isoforms share endoplasmic reticulum location, topology, and membrane-shaping properties. Plant Cell 22:1333-1343

Pubmed: [Author and Title](#)

CrossRef: [Author and Title](#)

Google Scholar: [Author Only](#) [Title Only](#) [Author and Title](#)

Tilney LG, Cooke TJ, Connelly PS, Tilney MS (1991) The structure of plasmodesmata as revealed by plasmolysis, detergent extraction, and protease digestion. J Cell Biol 112:739-747

Pubmed: [Author and Title](#)

CrossRef: [Author and Title](#)

Google Scholar: [Author Only](#) [Title Only](#) [Author and Title](#)

Tilsner J, Amari K, Torrance, L (2011) Plasmodesmata viewed as specialized membrane adhesion sites. Protoplasma 248 (1): 39-60

Pubmed: [Author and Title](#)

CrossRef: [Author and Title](#)

Google Scholar: [Author Only](#) [Title Only](#) [Author and Title](#)

Tilsner J, Linnik O, Louveaux M, Roberts IM, Chapman SN, Oparka KJ (2013) Replication and trafficking of a plant virus are coupled at the entrances of plasmodesmata. J Cell Biol 201(7):981-95

Pubmed: [Author and Title](#)

CrossRef: [Author and Title](#)

Google Scholar: [Author Only](#) [Title Only](#) [Author and Title](#)

Tolley N, Sparkes IA, Hunter PR, Craddock CP, Nuttall J, Roberts LM, Hawes C, Pedrazzini E, Frigerio L (2008) Overexpression of a plant reticulon remodels the lumen of the cortical endoplasmic reticulum but does not perturb protein transport. Traffic 8:94-102

Pubmed: [Author and Title](#)

CrossRef: [Author and Title](#)

Google Scholar: [Author Only](#) [Title Only](#) [Author and Title](#)

Tolley N, Sparkes I, Craddock CP, Eastmond PJ, Runions J, Hawes C, Frigerio L (2010) Transmembrane domain length is responsible for the ability of a plant reticulon to shape endoplasmic reticulum tubules in vivo. Plant J 64(3):411-8

Pubmed: [Author and Title](#)

CrossRef: [Author and Title](#)

Google Scholar: [Author Only](#) [Title Only](#) [Author and Title](#)

Vilar M, Sauri A, Monne M, Marcos JF, von Heijne G, Perez-Paya E, Mingarro I (2002) Insertion and topology of a plant viral movement protein in the endoplasmic reticulum membrane. J Biol Chem 277(26):23447-52

Pubmed: [Author and Title](#)

CrossRef: [Author and Title](#)

Google Scholar: [Author Only](#) [Title Only](#) [Author and Title](#)

Voeltz GK, Prinz WA, Shibata Y, Rist JM, Rapoport TA (2006) A class of membrane proteins shaping the tubular endoplasmic reticulum. Cell 124:573-586

Pubmed: [Author and Title](#)

CrossRef: [Author and Title](#)

Google Scholar: [Author Only](#) [Title Only](#) [Author and Title](#)

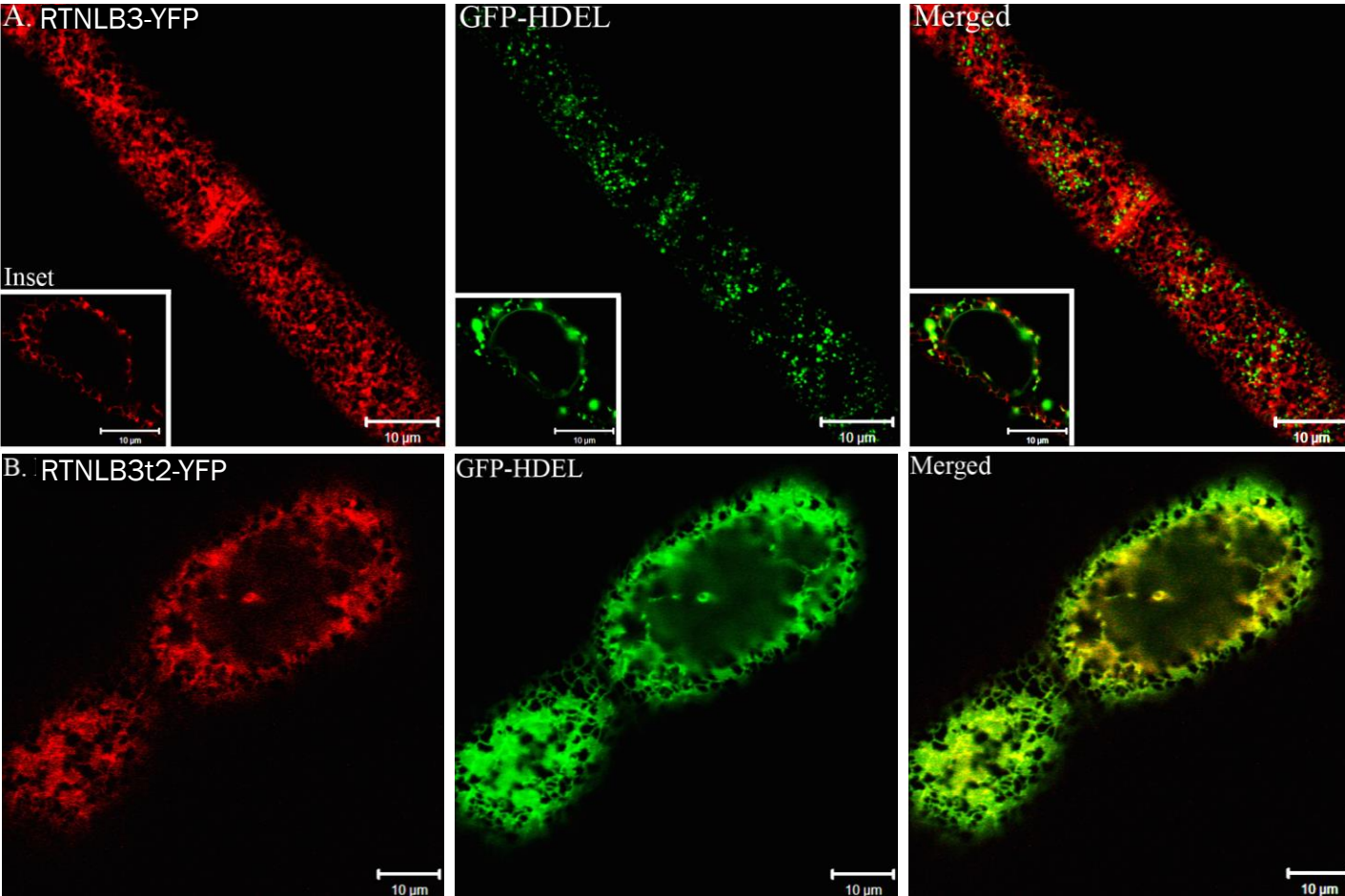
Wu ZY, Lee SC, Wang CW (2011) Viral protein targeting to the cortical endoplasmic reticulum is required for cell-cell spreading in plants. J Cell Biol 193(3):521-35

Pubmed: [Author and Title](#)

CrossRef: [Author and Title](#)

Google Scholar: [Author Only](#) [Title Only](#) [Author and Title](#)

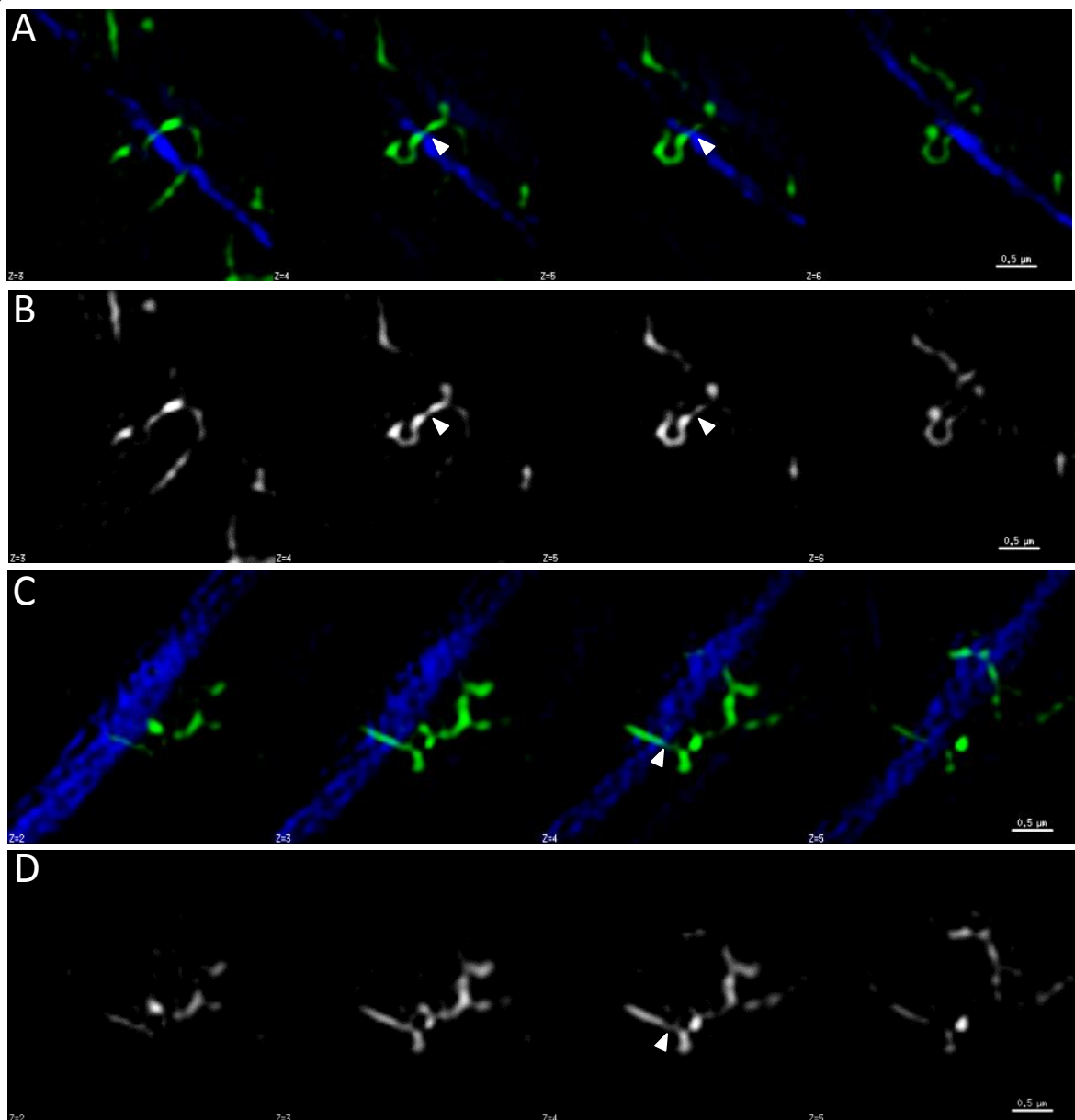
Figure S1



Supplementary Figure 1

RTNLB3-YFP can constrict the ER in interphase BY2 cells, whilst a truncated version cannot. A) GFP-HDEL is squeezed from the ER lumen into discrete luminal pockets when co-expressed with RTNLB3-YFP. Inset shows the nuclear envelope which has a low degree of curvature and is not labelled by RTNLB3. B) RTNLB3t2-YFP co-expressed with GFP-HDEL does not constrict the ER in BY2 cells.

Figure S2



Supplementary Figure 2

RTNLB6-GFP labels desmotubules in BY2 cells. Optical sections taken 150 nm apart in the axial dimension, show that a single desmotubule can be tracked as it crosses the cell wall. A and C) Series of sections showing RTNLB6-GFP (green) labelled ER is highly constricted as it passes through the cell wall (blue) B) Single channel of images in A or C, showing RTNLB6-GFP only. Bars = 0.5 μm .

Supplementary Video 1

Movie depicting a 3D reconstruction of ER (labelled with RTNLB6-GFP) associated with PD in BY2 cells.

Desmotubules can be seen as highly constricted regions crossing through the cell wall.